Sensing and Bio-Sensing Research 10 (2016) 27–33

Contents lists available at ScienceDirect

Sensing and Bio-Sensing Research

journal homepage: www.elsevier.com/locate/sbsr

Electrochemical detection of Hg(II) in water using self-assembled single walled carbon nanotube-poly(*m*-amino benzene sulfonic acid) on gold electrode

Gauta Gold Matlou [a], Duduzile Nkosi [a], Kriveshini Pillay [a], Omotayo Arotiba [a,b,*]

[a] Department of Applied Chemistry, University of Johannesburg, Doornfontein 2028, South Africa
[b] Centre for Nanomaterials Science Research, University of Johannesburg, Doornfontein 2028, South Africa

ARTICLE INFO

Article history:
Received 19 June 2016
Accepted 12 August 2016

Keywords:
Self-assembly
Gold electrode
Carbon nanotubes
Electrochemical detection
Mercury

ABSTRACT

This work reports on the detection of mercury using single walled carbon nanotube-poly (m-amino benzene sulfonic acid) (SWCNT-PABS) modified gold electrode by self-assembled monolayers (SAMs) technique. A thiol containing moiety (dimethyl amino ethane thiol (DMAET)) was used to facilitate the assembly of the SWCNT-PABS molecules onto the Au electrode surface. The successfully assembled monolayers were characterised using atomic force microscopy (AFM). Cyclic voltammetric and electrochemical impedance spectroscopic studies of the modified electrode (Au-DMAET-(SWCNT-PABS)) showed improved electron transfer over the bare Au electrode and the Au-DMAET in $[Fe(CN)_6]^{3-/4-}$ solution. The Au-DMAET-(SWCNT-PABS) was used for the detection of Hg in water by square wave anodic stripping voltammetry (SWASV) analysis at the following optimized conditions: deposition potential of −0.1 V, deposition time of 30 s, 0.1 M HCl electrolyte and pH 3. The sensor showed a good sensitivity and a limit of detection of 0.06 μM with a linear concentration range of 20 ppb to 250 ppb under the optimum conditions. The analytical applicability of the proposed method with the sensor electrode was tested with real water sample and the method was validated with inductively coupled plasma – optical emission spectroscopy.

1. Introduction

Mercury is a highly toxic metal in all its oxidation states (0, +1 and +2). It is emitted from natural sources (e.g. volcanic eruptions) and from anthropogenic sources like coal combustion and gold mining [1,2]. Mercury is very toxic to human where it causes abnormal functions of the brain, kidney, liver, eyes and bones upon accumulation in a body [3,4]. The toxicity of mercury at low level warrants its analysis in water and other samples [5] and also its removal from the environment [6].

Some of the methods developed for mercury detections incorporate the use of spectroscopic techniques such as atomic absorption spectroscopy (AAS), fluorescence spectroscopy (FS) and inductively coupled plasma spectroscopy (ICP). These methods are limited by their inapplicability on the sample site. Furthermore, they are expensive, require highly trained operating personnel, have high operating costs [7] and tedious sample preparations [8]. These shortcomings are made up for by electrochemistry methods which are low cost, and easier to operate in comparison to spectroscopic methods [7,9]. Among other electrochemistry methods, square wave anodic stripping voltammetry (SWASV) have been known to have excellent detection limits and selectivity's towards metal ion detection [10,11] in aqueous mediums [9]. SWASV have been applied in the detection of mercury [12] and other metals such as Pb, As and so on. In most cases, the electrodes used in SWASV are usually modified with other moieties so as to improve the stripping signal of the targeted metals. In this regards, the use of nanomaterials such as carbon nanotubes, carbon nanoparticles, gold, metal oxides, quantum dots, dendrimers etc. is not uncommon [13,14] Other electrode modifiers including organic films of conducting polymers and dendrimers have been reported. Carbon nanotubes (CNTs) and conductive polymers are known to possess excellent properties that are particularly useful in many fields. Polymer nanocomposites such as single walled carbon nanotube-poly amino benzene sulfonic acid (SWCNT-PABS) have a great synergy of properties from the polymer/CNTs structure. In electrochemical sensors, the CNTs provide the platforms with an advantage of small sizes and solutions required to deliver a response. The analysis are also carried at room temperature environment and provides high sensitivities with minute changes in electrical conductivity upon detection of the analyte [15].

The modification of electrodes is carried out by drop coating, electrodeposition, electropolymerization and self-assembled monolayers (SAMs) techniques. SAMs technique, is a coordinated chemical reaction that spontaneously create stable and well organized arrays of thin film

* Corresponding author at: Department of Applied Chemistry, University of Johannesburg, Doornfontein 2028, South Africa.
E-mail address: oarotiba@uj.ac.za (O. Arotiba).

http://dx.doi.org/10.1016/j.sbsr.2016.08.003

organic monolayers on substrate based on alternating adsorption of functional groups or complementary charges of materials [16–18]. SAMs of thiols has an advantage of resulting in systems (monolayers) of ordered, well packed and stable molecules on the gold solid substrate. The spontaneous formations of these systems are highly promoted by the strong gold-sulfur (Au—S) bonds formed between the thiol and the metallic gold surface and a further interaction between adjacent thiols through Van Der Waals forces. The resulting gold-SAMs surface has properties of both the attached thin film monolayers and the coinage metallic gold surface [19].

In this study, SWCNT-PABS are attached on the gold electrode surface using SAM technique facilitated by a thiol moiety (dimethyl amino ethane thiol) and used for the detection of Hg(II) in water using SWASV as an analytical tool for detection.

2. Experimental

2.1. Materials and apparatus

Mercury(II) nitrate monohydrate, 2-dimethyl amino ethane thiol hydrochloride (DMAET), Sulfuric acid, 30% Hydrogen peroxide, ethanol, Single walled carbon nanotubes-poly (m-amino benzene sulfonic acid) (SWCNT-PABS), potassium chloride, potassium ferricyanide (III), potassium hexacyanoferrate (II) trihydrate. A Three electrode system

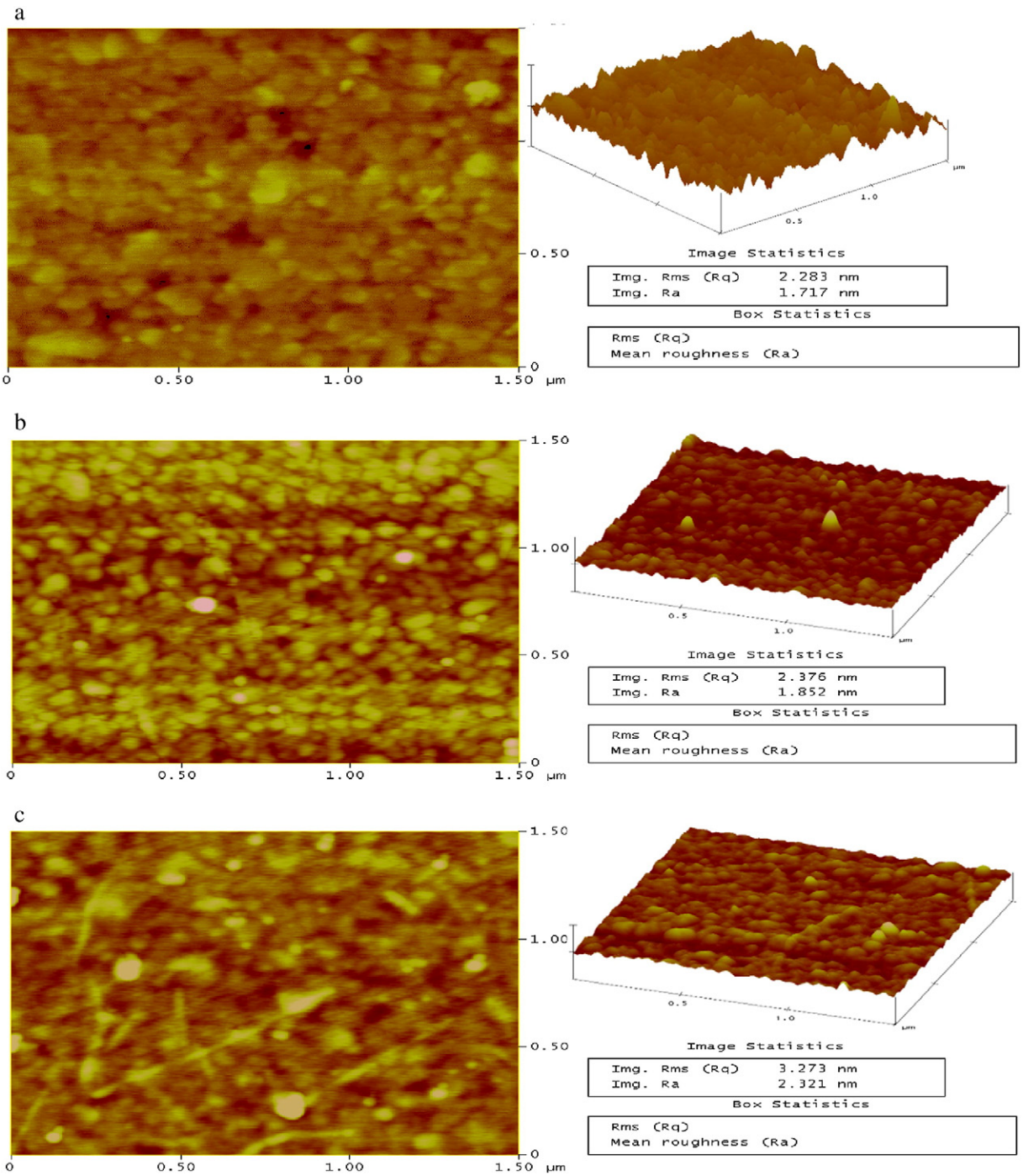

Fig. 1. 2D and the resultant 3D topographical surface images of the SAM modified gold disks at scan size of 1.5 µm. a) Bare Au surface. b) Au-DMAET surface. c) Au-DMAET-(SWCNT-PABS).

electrochemical workstation was used for electrochemical studies. A gold electrode ($r = 0.85$ mm, BAS, MF-2014) was used as a working electrode, a platinum wire electrode was used as a counter electrode and a Ag/AgCl (Bas, MF-2052 RE-5B) wire saturated in 3 M KCl was used as a pseudo reference electrode. Ultra-pure water with resistivity of 18.2 mΩ·cm obtained from Milli-Q Water system (Millipore Corp, Bedford, MA, USA) was used to prepare all solutions and electrode pretreatment.

2.2. Electrode pre-treatment and modification of the electrode surface

Prior to electrochemical application, the gold electrode was subjected to a sequence of mechanical, chemical and electrochemical cleaning [20,21]. Typically, the electrode was polished with alumina slurry (0.3 μm) and rinsed with ethanol and Millipore water for 10 min respectively. This was followed by dipping the electrode in a piranha solution (1 ml of 30% H_2O_2: 3 ml of Concentrated H_2SO_4) for 2 min, rinsed with ethanol and distilled water and finally conditioned with repeated cyclic scans between −0.15 V–1.6 V in 0.5 M H_2SO_4 at 50 mV/s for 20 scans or until a reproducible scan characteristic of a clean gold electrode is produced [22].

The cleaned electrode was modified using the SAMs technique as previously reported in literature [17,23]. The electrode was immersed in argon saturated 3 mM DMAET ethanol solution for 24 h to create the DMAET film on the electrode surface. It was then rinsed with ethanol to remove residual DMAET molecules (denoted as Au-DMAET modified electrode) and dried with argon gas. The Au-DMAET electrode was immersed in an argon saturated 1 mg/ml SWCNT-PABS water solution for 3 h, then rinsed with copious amounts of water and dried with argon gas to form the SWCNT-PABS film.

Veeco Dimension 3100 atomic force microscopy (AFM) coupled with Nanoscope V530r3sr3 software was used to confirm the attachment and topographical changes of the nanostructured films on the gold substrate. All AFM images were taken using the Eco-chemie SPR gold disks of 5 cm diameter with the AFM in tapping mode operation. Electrochemical experiments were performed using the Dropsens μstat 8000 equipped with Dropview 8400 software. Electrochemical impedance studies (EIS) were performed between 1.0 Hz to 10 kHz using a 5 mV rms sinusoidal modulation on a Compactstat electrochemical workstation (Ivium Technologies, Netherlands) with Ivium software. The EIS raw data was fitted using an equivalence fitting model available on the software.

2.3. Square wave anodic stripping voltammetric determination of Hg(II)

Square Wave Anodic Stripping Voltammetry (SWASV) was used as the analytical technique for the determination and detection of mercury in water samples using 0.1 M concentrations of HCl, NaCl, NaOH, H_2SO_4, and HNO_3 electrolytes. The pH of the electrolyte (HCl), the deposition potential and the deposition time were optimized while the $E_{conditioning}$ of 0.9 V, $t_{conditioning}$ of 10 s, relaxation time of 10 s, E_{amp} of 0.005 V, E_{step} of 0.002 V and frequency of 50 Hz were all kept constant throughout the stripping analysis. The proposed method was validated with inductively coupled plasma optical emission spectroscopy (ICP-OES). Selectivity of the sensor and the proposed method was tested against two fold concentrations of five common metallic cations (As(III), Cu(II), Cr(VI), Pb(II) and Cd(II)) that are found in water.

Owing to the incomplete removal of the mercury ions on the electrode surface during stripping which hinders linearity and reproducibility, an electrochemical cleaning procedure (de-stripping) was adopted as described in literature [24] and used to clean the electrode surface after each determination of mercury. This involved immersing the electrode in a blank solution (0.1 M HCl) and stripping at a positive potential (0.4 V) for 30 s to remove any residual mercury ions on the electrode surface. After every 10 stripping analysis of mercury, a new modified electrode was prepared following SAMs technique.

3. Results and discussions

3.1. Microscopic studies of the SAM modified surfaces

AFM was used to study and confirm the surface topographical changes as a result of the SAMs on a gold disk surface. Fig. 1 shows the 2D and the resultant 3D AFM images of the electrode modification at each assembly stage. The integration of monolayers on the gold substrate gave an increase in surface roughness (Img. Ra) and surface root mean square (Img. Rms) of the topographical make up as monolayers are added on the electrode surface. This trend is quite evident with the integration of the SWCNT-PABS monolayer on the Au-DMAET substrate surface where elongated nanotubes from the CNT can be seen on the 2D and 3D topographical images of the surface of the substrate (Fig. 1c). The addition of the alkane thiols (DMAET) on the bare Au surface did not result in significant changes on the surface (Fig. 1b) as compared with the addition of the SWCNT-PABS. The AFM study of the topographical surfaces suggested a well-defined integration of the monolayers on the gold solid surface. These topographical images are in agreement with the AFM images attained from similar studies conducted on the self-assembly of DMAET and SWCNT-PABS on gold surfaces [17,23,25].

3.2. Electrochemical characterisation of the SAM modified electrodes

The electrochemical responses of the gold electrode as a result of modification were interrogated by square wave voltammetry (SWV) and electrochemical impedance spectroscopy (EIS) (Fig. 2). From the SWV (Fig. 2a), the Au-DMAET electrode shows a lower current than

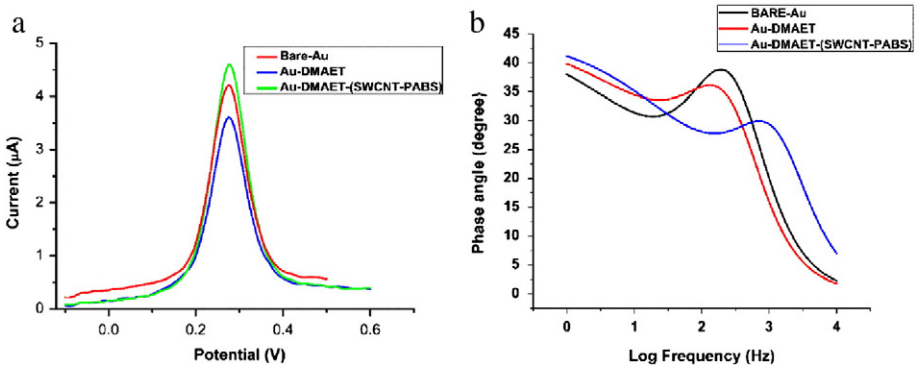

Fig. 2. Electrochemical studies of the SAM modified gold electrodes in equimolar solutions of 5 mM $[Fe(CN)_6]^{3-/4-}$ in 0.1 M KCl. A) SWV at 25 Hz frequency. B) Phase angle from electrochemical impedance spectroscopy.

Table 1
Summary of the EIS parameters of the SAMs modified electrodes with raw EIS fitted data percentage errors in brackets.

Electrode	Circuit parameters				
	R_S (Ω cm^2)	R_{CT} (Ω cm^2)	C1 (μF)	W1 (μΩsqrt Hz)	Phase angle (degree)
Bare Au	253.70 (1.17)	543.10 (0.87)	1.58 (1.43)	112.50 (0.24)	39
Au-DMAET	260.80 (1.33)	494.12 (3.69)	2.36 (8.86)	83.13 (0.19)	36
Au-DMAET-(SWCNT-PABS)	247.30 (1.23)	456.40 (1.51)	2.08 (2.01)	114.30 (0.26)	30

the bare gold electrode as expected because of the poor conductivity of the thin film of the DMAET which hindered the electron transfer rate of the redox probe. The highest current was observed after single walled carbon nanotubes-poly(*m*-amino benzene sulfonic acid) (SWCNT-PABS) was self-assembled on the Au-DMAET electrode. Firstly, this enhanced current is an indication of a successful assembly of the SWCNT-PABS on the DMAET. The linkage must have been enhanced by electrostatic attraction owing to the opposite charge of the positive DMAET and the negative SWCNT-PABS [19]. Secondly, the presence of SWCNT provided a larger surface area and improved the rate of electron transfer at the interface of the electrode and the redox probe. It has been shown that phase angle can be used as a measure the electron transfer kinetics at the electrode interface according to Eq. (1) where ϕ is the phase angle, R_s is the solution resistance and R_{ct} is the charge transfer resistance [26]

$$\phi = \tan^{-1}\left(\frac{1}{1+2R_sR_{ct}}\right) \quad (1)$$

According to Eq. (1), phase angle is directly proportional to charge transfer resistance. Thus phase angle decreases when there is a faster electron transfer at the electrode interface as seen in Fig. 2b and Table 1. The presence of SWNT enhanced the electron transfer of the ferrocyanide redox probe. The EIS result corroborates that of voltammetry. The charge transfer resistant obtained from the Nyquist plot (not shown) supports the trend observed from the phase angle (Table 1). The popular Randles equivalent circuit where electrolyte solution resistance (Rs) in series with a parallel combination of the double-layer capacitance C_{dl} and an impedance of a faradaic reaction (Rct (charge transfer resistance) and W1 (Warburg impedance)) was used to fit the impedance data obtained.

Surface coverages of the adsorbed monolayers on the Au electrode surface were calculated by first employing the Randles-Sevcik equation (Eq. (2)) to determine the effective area of the Au electrode surface for a reversible process in $[Fe(CN)_6]^{3-/4-}$ [27].

$$i_{pa} = \left(2.69\times10^5\right)n^{3/2}D^{1/2}\nu^{1/2}AC_0 \quad (2)$$

where *A* is the effective geometric area of the electrode surface, $D = 7.6\times10^{-5}\,cm^2s^{-1}$ is the diffusion coefficient of the $[Fe(CN)_6]^{3-/4-}$, C_0 is the bulk concentration of the redox probe [1 mM $[Fe(CN)_6]^{3-/4-}$], n = 1 is the number of the electrons transferred in the $[Fe(CN)_6]^{3-/4-}$

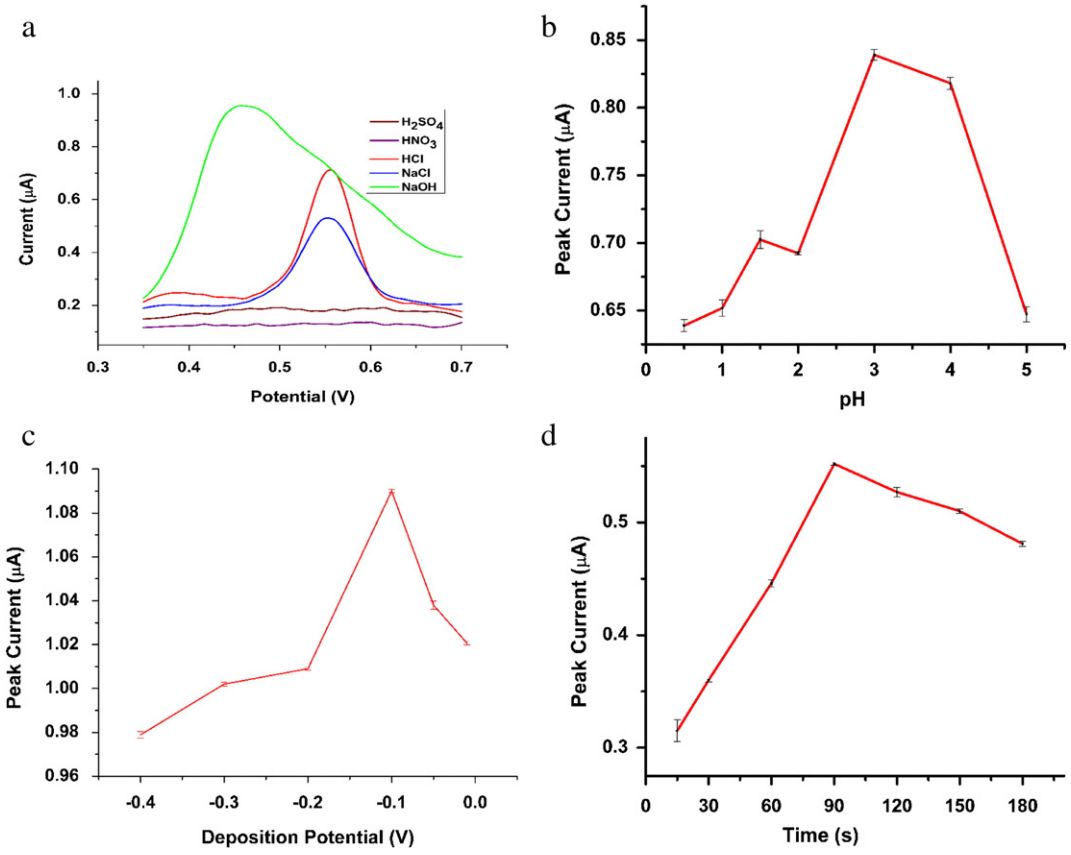

Fig. 3. Optimization of SWASV parameters for the detection of 100 ppb Hg(II) on the Au-DMAET-(SWCNT-PABS) electrode surface. a) Effect of electrolyte, b) Influence of pH, c) Effect of deposition potential and d) Effect of deposition time.

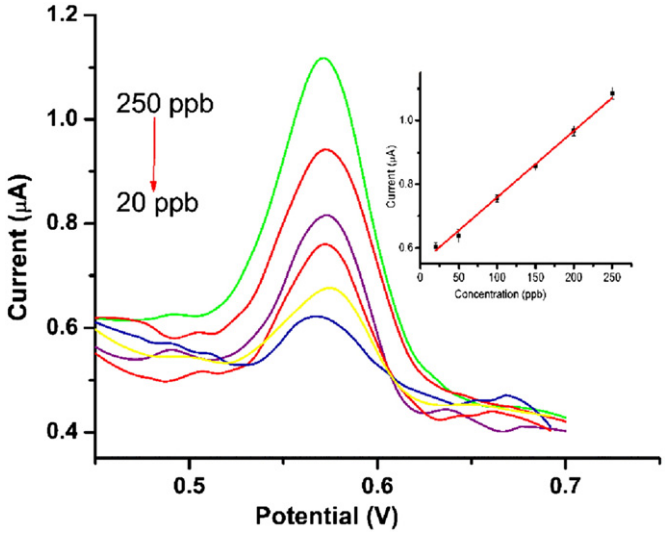

Fig. 4. SWASV Calibration curve of Hg(II) in 0.1 M HCl at different concentration (20 ppb–250 ppb) under optimum conditions. (Insert: peak current vs concentration depicting the linear relation).

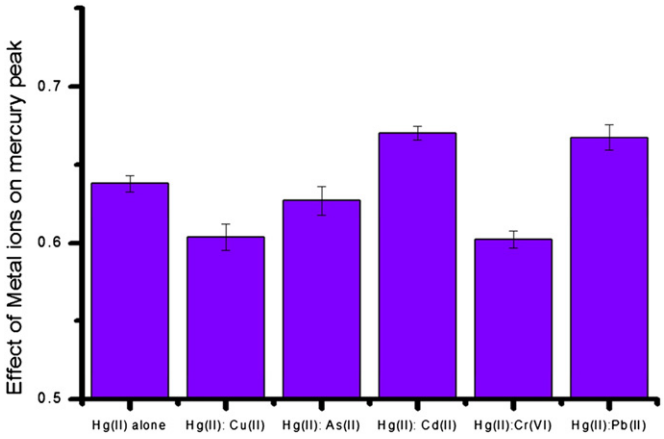

Fig. 5. Effect of the presence of common competing metal ions at two folds of concentration over the analyte concentration (2:1 ratio).

redox system while v is the scan rate. The effective area of the Au electrode surface was then found to be 0.00271 cm^2 which gave the surface roughness factor (ratio of the geometrical area to that of experimentally determined area) of 1.23. The surface coverage of the SAMs molecules on the electrode surface were then estimated using Eq. (3) as described in literature [28].

$$\Gamma_{SAMs} = \frac{Q}{nFA} \tag{3}$$

where Γ_{SAM} is the surface coverage achieved by the SAMs molecules on the electrode surface, Q (C) is the background corrected charge under the monolayer oxidation and reduction peaks, n = 1 is the number of the electrons transferred in the $[Fe(CN)_6]^{3-/4-}$ redox system, F = 96,485 C mol^{-1} is the Faradays constant and A = 0.0271 cm^2 is the effective area of the electrode surface [27]. The Γ_{SAMs} as found to be approximately 14.6840 μmol cm^{-2} for Au-DMAET and 17.4158 μmol cm^{-2} for Au-DMAET-(SWCNT-PABS) which shows increase in surface concentration of molecules on the electrode surface.

3.3. Square wave anodic stripping voltammetry of Hg(II) on Au-DMAET-(SWCNT-PABS)

3.3.1. Optimization of SWASV parameters

The parameters that affect the analysis of SWASV were optimized in order to improve the detection and the determination of Hg(II) in water (Fig. 3). Stripping analysis of Hg in different electrolytes were investigated (Fig. 3a) with HCl chosen as the electrolyte of choice owing to the well resolved peak current which was higher than all other electrolytes except NaOH. This choice of HCl could be attributed by the presence of chloride ions in solution that forms chlorocomplexes with mercury and promotes the mercury stripping peak to shift to a more negative potential while enhancing sensitivity and lowering the background currents [29]. Fig. 3b presents the effect of pH on the detection of Hg(II) on the Au-DMAET-(SWCNT-PABS). A peak current maxima occurred at pH 3 and this pH was chosen as the optimum pH for further analysis.

The investigation of the deposition potential and deposition time of Hg(II) stripping on the electrode surface is of utmost important because it facilitate the control of the mercury concentration on the electrode surface. This helps to control saturation and maintain linearity as loading increases [24]. For this reasons, deposition potentials (Fig. 3c) and deposition times (Fig. 3c) were investigated, with deposition potentials ranging from −0.01 V to −0.4 V and deposition times ranging from 15 s to 180 s. A deposition potential of −0.1 V gave the highest stripping peak in agreement with Wei et al. [30]. A time of 90 s was used as the optimum deposition time for stripping analysis of mercury.

3.3.2. Calibration plot for Hg(II) detection

Under the optimized parameters, a calibration curve was constructed by performing mercury stripping analysis under different concentrations of mercury in 0.1 M HCl (Fig. 4). The results gave linearity from 20 ppb to 250 ppb with a regression equation: y = 0.00205x + 0.5504 and a correlation coefficient of 0.9953. The limit of detection (LOD) was estimated using the equation described in literature [24] where $LOD = 3\sigma/m$ $LOD = \frac{3\delta}{m}$ $LOD = \frac{3\delta}{m}$ in which σ = standard deviation of the blank solution (0.1 M HCl) and the m is the slope of the linear equation. The LOD was estimated to be 0.0634 μM which is below the World Health Organisation (WHO) limit of 6 μM for inorganic mercury in drinking water. The LOD achieved by the proposed method was compared to other studies in Table 2. The low LOD indicates the sensitivity of the method with modified electrode and its potential use in analytical application. The reproducibility of the results was tested by 10 repetitive

Table 2
Electrochemical detection of mercury as reported by other authors.

Electrode	Method	Linear range	Detection limit	Reference
1) Au-DMAET-(SWCNT-PABS)	SWASV	20 μM − 250 μM	0.06 μM	This method
2) SWCNT-PhSH/Au	SWASV	5.0 nM–90 nM	3.0 nM	[30]
3) AuNPs/CFME	DPASV	0.2 μM − 50 μM	0.1 μM	[31]
4) AuNPs-GC	SWASV	0.64 μM–4 μM	0.42 μM	[32]
Cys-AuNPs-CILE	SWASV	10 nM–20 μM	2.3 μM	[33]
5) SPGE	SWASV	5 μM–30 μM	1.1 μM	[29]
6) np-AuNPs/ITO	DPASV	0.1 μM–10 μM	0.03 μM	[34]

SWASV (square wave anodic stripping voltammetry), DPASV (differential pulse anodic stripping voltammetry)

Table 3
Comparison of mercury concentrations (ppb) in water samples detected using ICP-OES and the proposed SWASV method (n = 3).

SAMPLE ID	ICP-OES	SWASV		
		Found	% Recovery	% RSD
Influent 1	2.22 ± 0.39	2.31 ± 0.09	112	5.9

stripping analysis of 10 ppb Hg(II) under the optimum conditions, which resulted in relative standard deviation (RSD) of 2.72%.

3.3.3. Interference studies of mercury

The influence of competing metal ions was investigated in two fold concentrations over the analyte i.e. 20 ppb interfering species: 10 ppb Hg in 0.1 M HCl. As(III), Cu(II), Cr(VI), Pb(II) and Cd(II) were used as competing metal ions and investigated individually against Hg(II). The results as illustrated in Fig. 5 shows Cu(II) and Cr(VI) as the predominant interfering species of mercury detection using the proposed SWASV method. The decrease of mercury stripping peak attained in the presence of Cu(II) and Cr(VI) could mean that the two metals have the ability to bind on the active sites of the modifier, this hindering the amount of mercury ions that binds on the modified electrode surface, subsequently causing a decrease on the stripping peak. Similar results were obtained with Cr as interfering species on Hg in a study conducted by Alves et al., 2011 [35]. In another study conducted by Punrat et al., 2014, the authors also found Cu(II) as a major interfering species at five folds concentrations of Hg(II) on gold-film screen-printed carbon electrode during stripping analysis [36]. Pb(II) and Cd(II) increased the peak current while As(III) did not have much effect on the detection of Hg(II). The mercury stripping peak increase in the presence of Pb(II) and Cd(II) could be as a result of overlapping stripping potential of metals on the electrode surface that cause an increase in stripping peak. These results (Fig. 5) indicate that the electrode is prone to interferences from these metals, which opens up a window for further studies to eliminate the interferences.

3.3.4. Detection of Hg in real water

To test the analytical applicability of the proposed method. A sample of influent water from a wastewater treatment plant in South Africa was taken. ICP-OES was used as a reference method on the same water samples. The water sample was spiked with 20 ppb Hg(II) during the mercury stripping measurement. The pre-treatment of the water samples involved treatment with 1% of nitric acid and filtering with 0.45 μ micro syringe filter. SWASV was performed on water samples containing 0.1 M HCl under the optimum parameters of the proposed method. The analysis (Table 3) shows agreement between the results obtained from the two methods. These results validate the excellent potential analytical applicability of the proposed method with the electrode.

4. Conclusion

This work describes another application of self-assembled monolayer in the preparation of a modified electrode for sensor application. The Au-DMAET-(SWCNT-PABS) electrode was used for the detection of Hg(II) using SWASV. The analytical relevance of the reported method can be supported by i) the detection limit which is lower than the WHO permissible limit of Hg in water; ii) its application in real water sample and iii) its validation with ICP-OES. Thus this method can be used for the detection of other metallic species in water.

Acknowledgements

The authors express gratitude to the following for funding: National Nanoscience Postgraduate Teaching and Training Platform (NNPTTP) of South Africa; Centre for Nanomaterials Science Research, University of Johannesburg, South Africa; The National Research Foundation of South Africa Thuthuka Grant numbers TTK150709124795 and 88066; Water Research Commission, South Africa Grant Number: K5/2387. Our appreciation also goes to the Microscopy and Microanalysis unit (MMU) of the University of the Witwatersrand in Johannesburg, South Africa for the permission to use Veeco Atomic Force Microscope.

References

[1] K. Pillay, E.M. Cukrowska, N.J. Coville, Improved uptake of mercury by Sulphur-containing carbon nanotubes, Microchem. J. 108 (2013) 124–130.
[2] S.L.C. Ferreira, V.A. Lemos, L.O.B. Silva, A.F.S. Queiroz, A.S. Souza, E.G.P. da Silva, W.N.L. dos Santos, C.F.d. Virgens, Analytical strategies of sample preparation for the determination of mercury in food matrices - a review, Microchem. J. 121 (2015) 227–236.
[3] G. Aragay, A. Merkoc, Nanomaterials application in electrochemical detection of heavy metals, Electrochim. Acta 84 (2012) 49–61.
[4] G.V. Ramesh, T.P. Radhakrishnan, A universal sensor for mercury (Hg, Hg I , Hg II) based on silver nanoparticle-embedded polymer thin film, Appl. Mater. Interfaces 3 (2011) 988–994.
[5] L. Cui, J. Wu, H. Ju, Electrochemical sensing of heavy metal ions with inorganic, organic and bio-materials, Biosens. Bioelectron. 63 (2015) 276–286.
[6] C. Zhang, J. Sui, J. Li, Y. Tang, W. Cai, Efficient removal of heavy metal ions by thiol-functionalized superparamagnetic carbon nanotubes, Chem. Eng. J. 210 (2012) 45–52.
[7] Y.-R. Kim, R.K. Mahajan, J.S. Kim, H. Kim, Highly sensitive gold nanoparticle-based colorimetric sensing of mercury(II) through simple ligand exchange reaction in aqueous media, ACS Appl. Mater. Interfaces 2 (2010) 292–295.
[8] D. Liu, W. Qu, W. Chen, W. Zhang, Z. Wang, X. Jiang, Letters to analytical chemistry highly sensitive, colorimetric detection of mercury (II) in aqueous media by quaternary ammonium group-capped gold nanoparticles at room temperature, Anal. Chem. 82 (2010) 9606–9610.
[9] Z. Wang, H. Wang, Z. Zhang, X. Yang, G. Liu, Sensitive electrochemical determination of trace cadmium on a stannum film/poly(p-aminobenzene sulfonic acid)/electrochemically reduced graphene composite modified electrode, Electrochim. Acta 120 (2014) 140–146.
[10] T. Ndlovu, B.B. Mamba, S. Sampath, R.W. Krause, O.A. Arotiba, Voltammetric detection of arsenic on a bismuth modified exfoliated graphite electrode, Electrochim. Acta 128 (2014) 48–53.
[11] G.D. Pierini, M.F. Pistonesi, M.S. Di Nezio, M.E. Centurión, A pencil-lead bismuth film electrode and chemometric tools for simultaneous determination of heavy metals in propolis samples, Microchem. J. 125 (2016) 266–272.
[12] P.J. Mafa, A.O. Idris, N. Mabuba, O.A. Arotiba, Electrochemical co-detection of as(III), Hg(II) and Pb(II) on a bismuth modified exfoliated graphite electrode, Talanta 153 (2016) 99–106.
[13] T. Ndlovu, A.T. Kuvarega, O.A. Arotiba, S. Sampath, R.W. Krause, B.B. Mamba, Exfoliated graphite/titanium dioxide nanocomposites for photodegradation of eosin yellow, Appl. Surf. Sci. 300 (2014) 159–164.
[14] K. Lawrence, C.L. Baker, T.D. James, S.D. Bull, R. Lawrence, J.M. Mitchels, M. Opallo, O.A. Arotiba, K.I. Ozoemena, F. Marken, Functionalized carbon nanoparticles, blacks and soots as electron-transfer building blocks and conduits, Chem. Asian J. 9 (2014) 1226–1241.
[15] J.-K. Kim, Application of CNT/Polymer Nanocomposites, in: F.-C. Ma, J.-K. Kim (Eds.), Carbon Nanotub. Polym. Reinf, 1st edCRC Press, New York 2011, pp. 169–191.
[16] J. Pillay, K.I. Ozoemena, Layer-by-layer self-assembled nanostructured phthalocyaninatoiron(II)/SWCNT-poly(m-aminobenzenesulfonic acid) hybrid system on gold surface: electron transfer dynamics and amplification of H_2O_2 response, Electrochim. Acta 54 (2009) 5053–5059.
[17] J. Pillay, B.O. Agboola, K.I. Ozoemena, Electrochemistry of 2-dimethylaminoethanethiol SAM on gold electrode: interaction with SWCNT-poly(m-aminobenzene sulphonic acid), electric field-induced protonation–deprotonation, and surface pKa, Electrochem. Commun. 11 (2009) 1292–1296.
[18] K.I. Ozoemena, T. Nyokong, D. Nkosi, I. Chambrier, M.J. Cook, Insights into the surface and redox properties of single-walled carbon nanotube—cobalt(II) tetraaminophthalocyanine self-assembled on gold electrode, Electrochim. Acta 52 (2007) 4132–4143.
[19] J. Meena Devi, A simulation study on the thermal and wetting behavior of alkane thiol SAM on gold (111) surface, Prog. Nat. Sci. Mater. Int. 24 (2014) 405–411.
[20] L.M. Fischer, M. Tenje, A.R. Heiskanen, N. Masuda, J. Castillo, A. Bentien, J. Émneus, M.H. Jakobsen, A. Boisen, Gold cleaning methods for electrochemical detection applications, Microelectron. Eng. 86 (2009) 1282–1285.
[21] G. Dutta, K. Jo, H. Lee, B. Kim, H. Young, H. Yang, Time-dependent decrease in the enhanced electrocatalytic activities observed after three different pretreatments of gold electrodes, J. Electroanal. Chem. 675 (2012) 41–46.
[22] Z. Li, L. Zhang, S. Zeng, M. Zhang, E. Du, B. Li, Effect of surface pretreatment on self-assembly of thiol-modified DNA monolayers on gold electrode, J. Electroanal. Chem. 722-723 (2014) 131–140.
[23] J. Pillay, K.I. Ozoemena, Layer-by-layer self-assembled nanostructured phthalocyaninatoiron (II)/SWCNT-poly (m-aminobenzenesulfonic acid) hybrid system on gold surface: electron transfer dynamics and amplification of H_2O_2 response, Electrochim. Acta 54 (2009) 5053–5059.

[24] A. Giacomino, O. Abollino, M. Malandrino, E. Mentasti, Parameters affecting the determination of mercury by anodic stripping voltammetry using a gold electrode, Talanta 75 (2008) 266–273.
[25] B.O. Agboola, J. Pillay, K. Makgopa, K.I. Ozoemena, Electrochemical characterization of mixed self-assembled films of water-soluble single-walled carbon nanotube-poly(m-aminobenzene sulfonic acid) and iron(II) tetrasulfophthalocyanine, J. Electrochem. Soc. 157 (2010) F159.
[26] O.A. Arotiba, P.G. Baker, B.B. Mamba, E.I. Iwuoha, The application of electrodeposited poly(propylene imine) dendrimer as an immobilisation layer in a simple electrochemical DNA biosensor, Int. J. Electrochem. Sci. 6 (2011) 673–683.
[27] A.J. Bard, L.R. Faulkner, E. Swain, C. Robey, Electrochemical Methods: Fundamentals and Applications, Second ed. John Wiley and Sons, Inc, New York, 2001.
[28] V.P. Chauke, E. Antunes, T. Nyokong, Comparative behavior of conjugates of tantalum phthalocyanines with gold nanoparticles or single walled carbon nanotubes towards bisphenol A electrocatalysis, J. Electroanal. Chem. 661 (2011) 1–7.
[29] E. Bernalte, C.M. Sánchez, E.P. Gil, Determination of mercury in ambient water samples by anodic stripping voltammetry on screen-printed gold electrodes, Anal. Chim. Acta 689 (2011) 60–64.
[30] J. Wei, D. Yang, H. Chen, Y. Gao, H. Li, Stripping voltammetric determination of mercury(II) based on SWCNT-PhSH modified gold electrode, Sensors Actuators B Chem. 190 (2014) 968–974.
[31] D. Li, J. Li, X. Jia, E. Wang, Gold nanoparticles decorated carbon fiber mat as a novel sensing platform for sensitive detection of Hg(II), Electrochem. Commun. 42 (2014) 30–33.
[32] T. Hezard, K. Fajerwerg, D. Evrard, V. Collire, P. Behra, P. Gros, Gold nanoparticles electrodeposited on glassy carbon using cyclic voltammetry: application to Hg(II) trace analysis, J. Electroanal. Chem. 664 (2012) 46–52.
[33] A. Safavi, E. Farjami, Construction of a carbon nanocomposite electrode based on amino acids functionalized gold nanoparticles for trace electrochemical detection of mercury, Anal. Chim. Acta 688 (2011) 43–48.
[34] Y. Lin, Y. Peng, J. Di, Electrochemical detection of Hg(II) ions based on nanoporous gold nanoparticles modified indium tin oxide electrode, Sensors Actuators B Chem. 220 (2015) 1086–1090.
[35] G.M.S. Alves, J.M.C.S. Magalhães, P. Salaün, C.M.G. Van Den Berg, H.M.V.M. Soares, Simultaneous electrochemical determination of arsenic, copper, lead and mercury in unpolluted fresh waters using a vibrating gold microwire electrode, Anal. Chim. Acta 703 (2011) 1–7.
[36] E. Punrat, S. Chuanuwatanakul, T. Kaneta, S. Motomizu, O. Chailapakul, Method development for the determination of mercury (II) by sequential injection/anodic stripping voltammetry using long-lasting gold-modified screen-printed carbon electrode, J. Electroanal. Chem. 727 (2014) 78–83.